JOURNAL OF MATERIALS SCIENCE 22 (1987) 4550–4557

Crystallization kinetics of some iron-based metallic glasses

M. A. GIBSON, G. W. DELAMORE
Department of Metallurgy and Materials Engineering, University of Wollongong, Wollongong, New South Wales 2500, Australia

The crystallization behaviour of a range of iron-based metallic glasses has been examined by isothermal differential scanning calorimetry, optical and transmission electron microscopy. It was found that the conventional procedure of applying the Johnson–Mehl–Avrami equation to determine reaction mechanisms, i.e. calculating a mean value of the Avrami exponent over a range of volume fraction transformed, can be misleading. The technique suggested by Calka and Radlinski, when used in conjunction with detailed metallography, is shown to be a more sensitive and reliable indicator of reaction mechanisms.

1. Introduction

The Johnson–Mehl–Avrami (JMA) equation has been used extensively to analyse the crystallization kinetics of a wide range of metallic glass systems [1–8]. The equation is usually written

$$x(t) = 1 - \exp[-K(t - \tau)^n]$$

where $x(t)$ is the volume fraction transformed in time t, K is a rate constant, τ is the incubation period before the transformation begins and n is the Avrami exponent which reflects the nucleation and/or growth characteristics of the transformation. For isothermal crystallization, a plot of $\ln[-\ln(1 - x)]$ against $\ln(t - \tau)$ should give a straight line, the slope of which represents the Avrami exponent. If the JMA analysis is valid, the value of n should not change with either the volume fraction transformed, V_f, or the temperature of transformation.

A recent paper by Calka and Radlinski [9] has shown that the usual method of applying the JMA equation, i.e., calculating a mean value of the Avrami exponent over a range of volume fraction transformed, may be inappropriate, even misleading, if competing reactions or changes in growth dimensionality occur during the progress of the transformation. Although most of the published work on the crystallization of metallic glasses suggests that correlation coefficients of 0.99 or better result from the calculation of a mean value of n, a close examination of the Avrami plots reveals that there are deviations from linearity over the full range of volume fraction transformed. A more sensitive approach is to plot the first derivative of the Avrami plot against the volume fraction transformed [9, 10] which effectively gives the local value of n with V_f. Such a plot, called here a Calka plot for convenience, allows a more detailed appraisal of the data and can highlight changes in reaction kinetics during the progress of the transformation.

The literature on crystallization of iron-based metallic glasses shows a wide variation in values of the mean Avrami exponent obtained from differential scanning calorimetry (DSC), [11–20], resistivity measurements [21–24], Mössbauer effect spectroscopy [25] and microstructural studies [26, 27], even for the same alloy compositions. The present investigation, which is part of a wider study, was directed at applying the analysis technique suggested by Calka and Radlinski to a range of iron-based metallic glasses in an attempt to resolve some of the variability in the literature.

2. Experimental procedure

A series of iron-based alloys was prepared from high purity components. The constituents were melted together in sealed quartz tubes under an argon atmosphere and subsequently homogenized by remelting several times on a water-cooled copper hearth in an arc furnace. Metallic glass ribbons approximately 5 mm wide and 25 to 30 μm thick were melt-spun in air on a stainless steel wheel 300 mm in diameter rotating at 2500 r.p.m. The ribbons were checked for lack of crystallinity by X-ray diffraction from both surfaces and by transmission electron microscopy (TEM), on electrochemically thinned foils.

Dynamic DSC using a Mettler TA 3000 system was used to characterize the crystallization behaviour of each of the alloys and to determine suitable temperature ranges for isothermal annealing. For the isothermal experiments, the DSC furnace was set to the required temperature before insertion of the specimen. All the DSC work was carried out in a flowing argon atmosphere.

Partially crystallized specimens were mounted in cold-setting resin and polished for metallographic examination. Foils were prepared for TEM examination by electrochemical thinning in a Struers Tenupol twin jet polisher.

3. Results

3.1. Dynamic DSC

Of the alloys examined, four displayed a single, sharp

0022–2461/87 $03.00 + .12

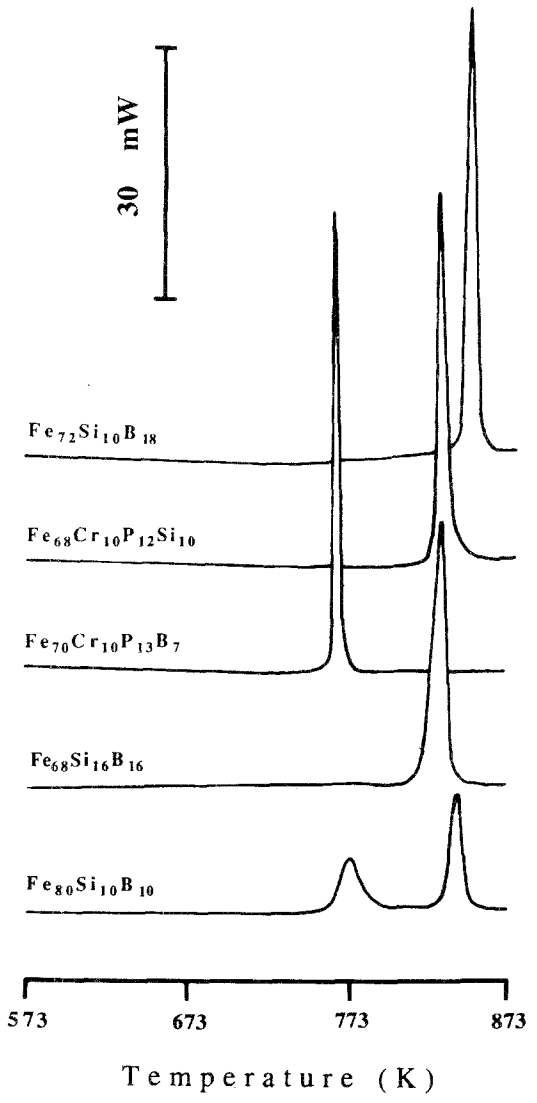

Figure 1 DSC thermograms from dynamic runs at 20 K min^{-1}.

exothermic peak, $Fe_{72}Si_{10}B_{18}$, $Fe_{68}Si_{16}B_{16}$, $Fe_{70}Cr_{10}P_{13}B_7$, and $Fe_{68}Cr_{10}P_{12}Si_{10}$, while $Fe_{80}Si_{10}B_{10}$ showed a double crystallization peak (Fig. 1).

3.2. Isothermal DSC

It was found that the alloys could be divided into two groups depending on their DSC response on isothermal heating. The first group includes those alloys for which a substantial incubation period was detected prior to crystallization and which gave flat, coincident baselines both before and after crystallization was complete. Fig. 2 shows DSC traces typical of this group of alloys. The second group comprises those alloys where the transformation began during the instrument transient, irrespective of the annealing temperature selected (Fig. 3).

3.2.1. Group 1 alloys

Ribbons of $Fe_{68}Cr_{10}P_{12}Si_{10}$ produced a single bell-shaped DSC peak on isothermal annealing which was readily analysed in the conventional manner. The single peak for $Fe_{68}Si_{16}B_{16}$ was slightly skewed towards longer times but analysis was again straightforward.

$Fe_{80}Si_{10}B_{10}$ crystallizes by a two-stage process and it was found that each stage could be analysed separately using a double annealing treatment [18, 20]. This involves transforming the sample at low temperatures through the first stage of transformation until a flat baseline is obtained, removing the sample and cooling rapidly to room temperature, resetting the furnace to an appropriate higher temperature and replacing the sample for analysis of the second stage of the transformation. Detailed analysis of this procedure [28] has shown that the first stage annealing treatment does not affect the progress of the second stage. The first peak in this alloy was asymmetric, being skewed towards longer times, whilst the higher temperature peak was more symmetrical, similar to that of $Fe_{68}Cr_{10}P_{12}Si_{10}$.

3.2.2. Group 2 alloys

The experimental results for alloys in this group, $Fe_{70}Cr_{10}P_{13}B_7$ and $Fe_{72}Si_{10}B_{18}$, could not be analysed directly because of the lack of a flat initial baseline, indicating that the start of the transformation occurred during the settling time of the instrument. In order to overcome this problem, the instrumental transient was determined by separate isothermal runs at each of the temperatures of interest using an equal amount of a glassy alloy of greater thermal stability, i.e. one which showed a substantial incubation period. The resulting curves for the instrumental transient were then subtracted from the experimental plots for each of the alloys as shown in Fig. 4. The effect of this correction is very slight, particularly at the lower annealing temperatures; the majority of the thermogram remains unaffected.

The plots of volume fraction transformed against time for all of these alloys were of the usual sigmoidal

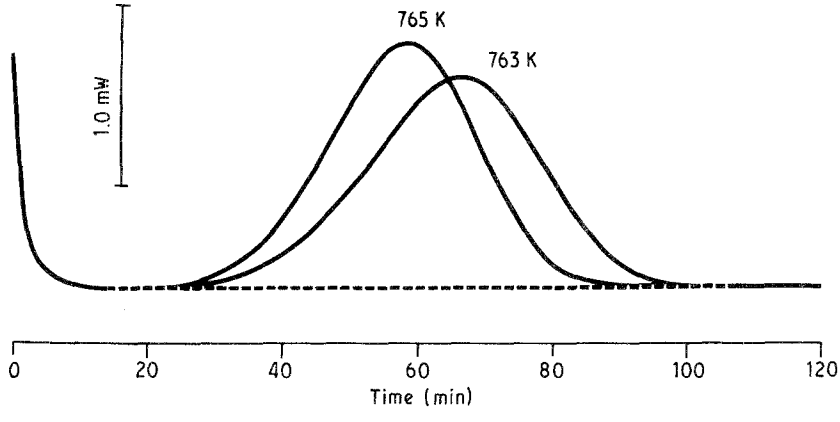

Figure 2 Isothermal DSC thermograms for $Fe_{68}Cr_{10}P_{12}Si_{10}$. Note the substantial incubation period and symmetrical peaks.

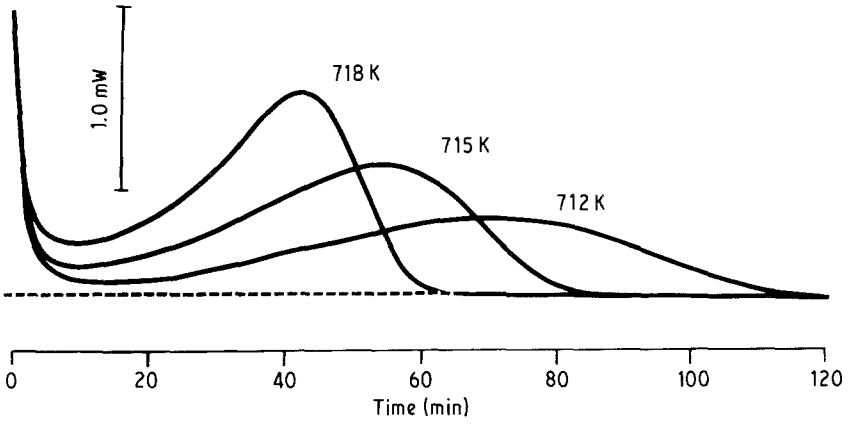

Figure 3 Isothermal DSC thermograms for $Fe_{70}Cr_{10}P_{13}B_7$. The peaks are skewed to shorter times and there is no incubation period prior to the onset of crystallization.

form. The mean Avrami exponents for each of the experimental curves were determined from the slopes of the $\ln[-\ln(1-x)]$ against $\ln(t)$ plots over the range 0.10 to 0.90 volume fraction transformed and are listed in Table I. Examples of Avrami plots typical of both groups of alloys are shown in Figs 5 and 6. The variation of n with V_f was investigated by plotting $\delta\{\ln[-\ln(1-x)]\}/\delta \ln(t-\tau)$ against volume fraction transformed at each temperature and the results given in Figs 7 to 12.

Optical and transmission electron micrographs of representative areas from a selection of the alloys investigated are shown in Figs 13 to 17.

4. Discussion

The results illustrate clearly the value of the Calka plot and the importance of complementary metallographic studies in work concerned with crystallization kinetics. It is apparent that calculation of a mean value of the Avrami exponent over a range of volume fraction transformed, even when high values of correlation coefficient result from the analysis, may be quite misleading if such mean values are used to infer crystallization mechanisms.

4.1. Group 1 alloys

Ribbons of $Fe_{68}Cr_{10}P_{12}Si_{10}$ at each annealing temperature gave a mean value of n of approximately 4.0, suggesting three-dimensional, interface-controlled growth with constant nucleation rate [29]. The Calka plots confirmed that the Avrami exponent remained constant at around 4.0 over the majority of the transformation, irrespective of the transformation temperature (Fig. 7). Deviations at low V_f reflect the experimental difficulty in determining the exact time of start of the transformation and the exaggerated effect that this has on the calculation of V_f, while deviations at high V_f are due to the ultimately limiting effect of the ribbon surfaces. Microstructural examination showed that crystallization occurred uniformly throughout the ribbon cross-section with no evidence of preferred growth from the surfaces. TEM investigation of thin foils showed that the crystallization product was two-phase (Fig. 13), supporting the kinetic evidence for interface-controlled growth.

The Avrami plots for $Fe_{68}Si_{16}B_{16}$ gave a mean n value of 3.0 which suggests three-dimensional, interface-controlled growth with zero nucleation rate, i.e. growth from quenched-in nuclei. The Calka plot confirmed that the mean value of n in this case also was genuinely representative of the crystallization process (Fig. 8), as did the metallographic evidence which shows uniformly distributed growth sites throughout the ribbon (Fig. 14). The crystallization product was again two-phase. It should be noted that this alloy composition lies close to the glass-forming boundary in the FeSiB system [30] and the evidence for quenched-in nuclei probably reflects the difficulty in obtaining completely amorphous ribbons at this composition.

Results for the $Fe_{80}Si_{10}B_{10}$ alloy show clearly that under appropriate conditions metallic glasses which crystallize in multiple stages can be analysed as readily

TABLE I Kinetic data from Avrami analysis

Composition	Annealing temperature (K)	Mean n	Correlation coefficient
$Fe_{68}Cr_{10}P_{12}Si_{10}$	763	3.95	0.9999
	765	4.01	0.9999
$Fe_{68}Si_{16}B_{16}$	759	3.01	0.9999
	767	3.00	0.9999
$Fe_{80}Si_{10}B_{10}$ (first peak)	704	2.51	0.9998
	708	2.49	0.9998
$Fe_{80}Si_{10}B_{10}$ (second peak)	765	3.95	0.9999
	769	3.97	0.9999
	773	4.01	0.9999
$Fe_{72}Si_{10}B_{18}$	793	2.72	0.9964
	798	3.23	0.9962
$Fe_{70}Cr_{10}P_{13}B_7$	712	2.76	0.9975
	715	2.97	0.9951
	718	3.30	0.9923

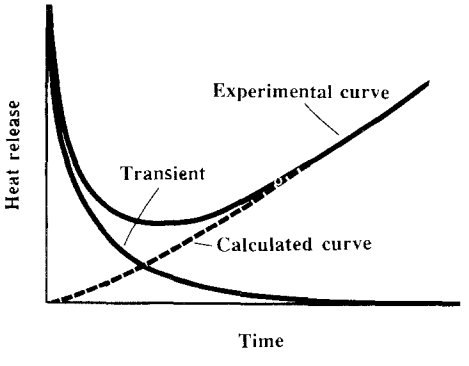

Figure 4 Schematic diagram showing the construction of a working curve for those alloys in which no incubation period was observed.

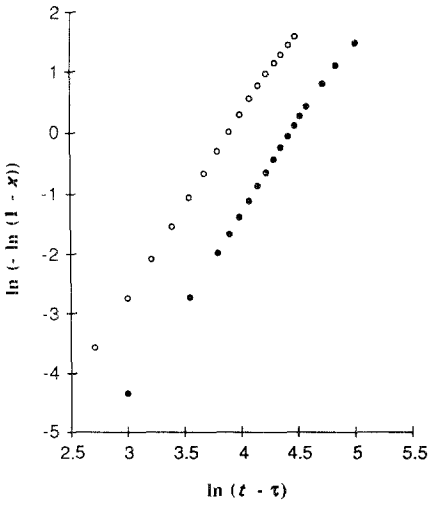

Figure 5 Avrami plot for $Fe_{68}Si_{16}B_{16}$, typical of Group 1 alloys. (●) 759 K, (○) 767 K.

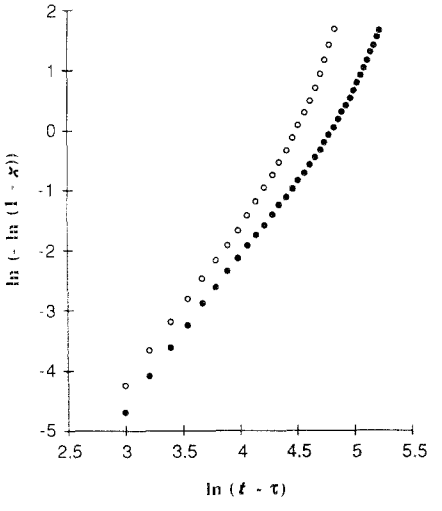

Figure 6 Avrami plot for $Fe_{72}Si_{10}B_{18}$, typical of Group 2 alloys. (●) 793 K, (○) 798 K.

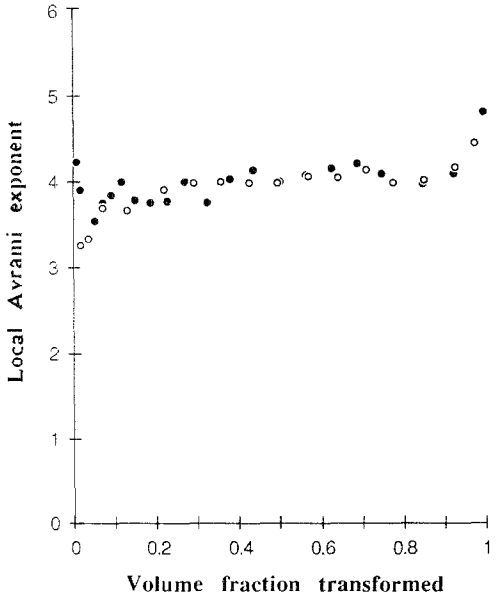

Figure 7 The variation in local value of Avrami exponent with volume fraction transformed (Calka plot), for $Fe_{68}Cr_{10}P_{12}Si_{10}$. (●) 763 K, (○) 765 K.

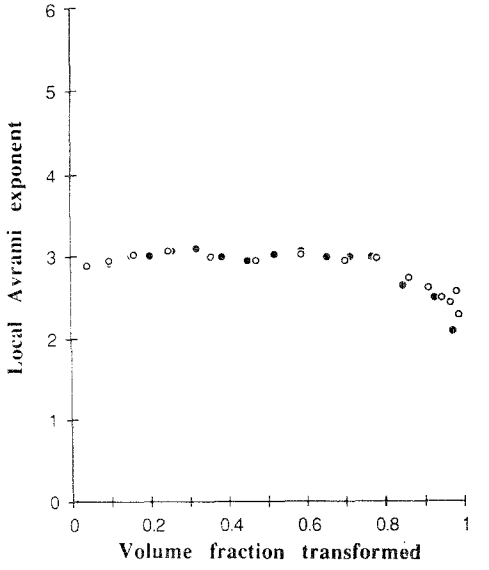

Figure 8 The variation in local value of Avrami exponent with volume fraction transformed (Calka plot), for $Fe_{68}Si_{16}B_{16}$. (●) 759 K, (○) 767 K.

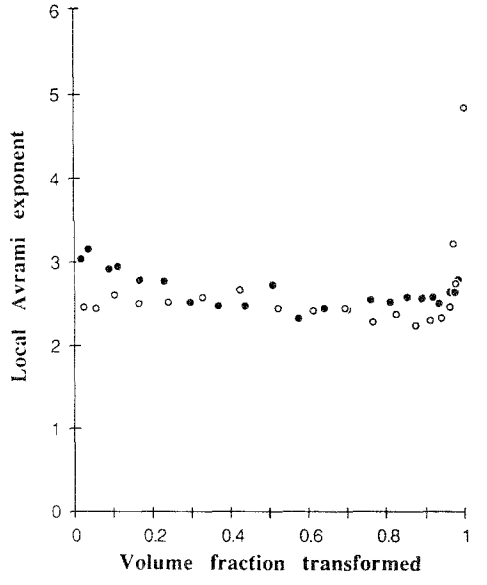

Figure 9 The variation in local value of Avrami exponent with volume fraction transformed (Calka plot), for $Fe_{80}Si_{10}B_{10}$ (first peak). (●) 704 K, (○) 708 K.

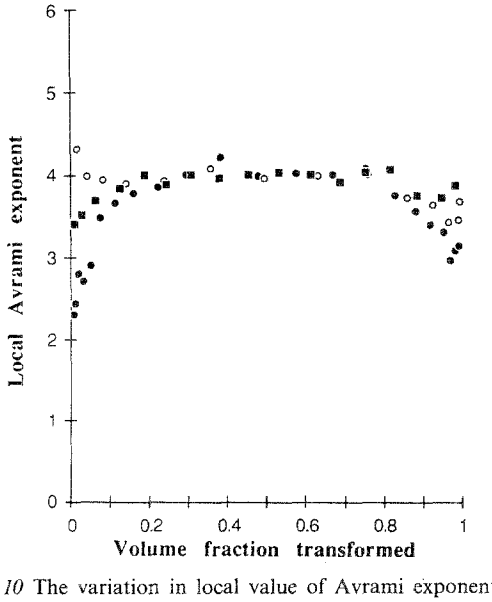

Figure 10 The variation in local value of Avrami exponent with volume fraction transformed (Calka plot), for $Fe_{80}Si_{10}B_{10}$ (second peak). (●) 765 K, (○) 769 K, (■) 773 K.

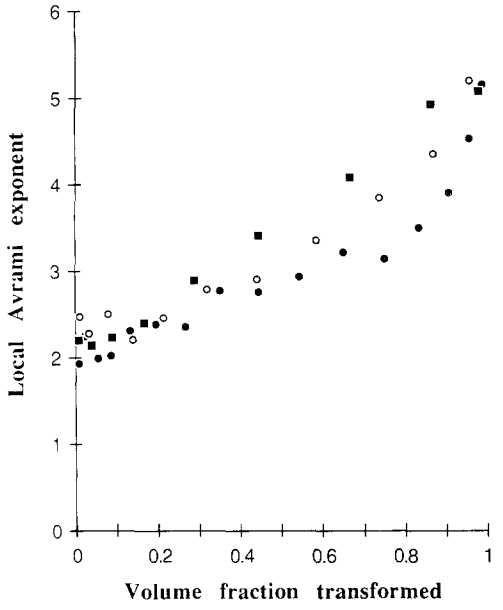

Figure 11 The variation in local value of Avrami exponent with volume fraction transformed (Calka plot), for $Fe_{70}Cr_{10}P_{13}B_7$. (●) 712 K, (○) 715 K, (■) 718 K.

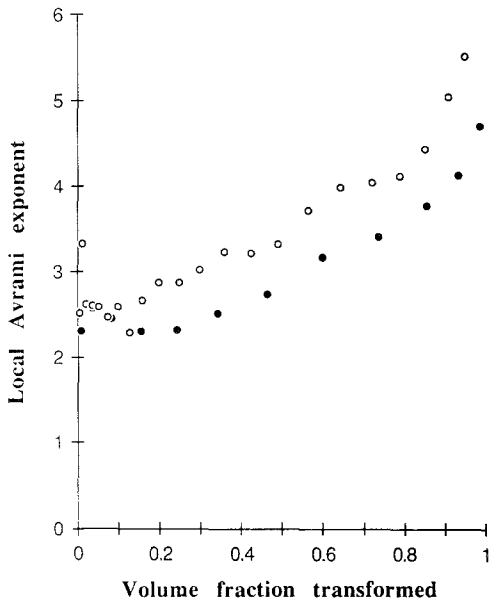

Figure 12 The variation in local value of Avrami exponent with volume fraction transformed (Calka plot), for $Fe_{72}Si_{10}B_{18}$. (●) 793 K, (○) 798 K.

as those which produce only single-stage transformations. The first stage in this alloy gave a mean n value of 2.5 (three-dimensional, diffusion-controlled growth with a constant nucleation rate), while the second stage was characterized by a mean n value of 4.0. Calka plots (Figs 9 and 10) showed that for each stage the transformation was correctly given by the mean value and the microstructural evidence (Fig. 15) confirmed the values of 2.5 – uniformly distributed dendritic crystals – and 4.0 – uniformly distributed two-phase cells growing independently of the first stage dendrites. Other hypoeutectic FeSiB alloys which crystallize by a two-stage process have also been shown to have mean n values of 2.5 and 4.0 for the individual steps: these results will be presented elsewhere.

4.2. Group 2 alloys

Both alloys in this group gave mean n values which varied with temperature and the Calka plots showed that n increased steadily with volume fraction transformed over the complete range, generally from around 2 up to 4 or higher (Figs 11 and 12). The microstructures of both alloys were similar: in each

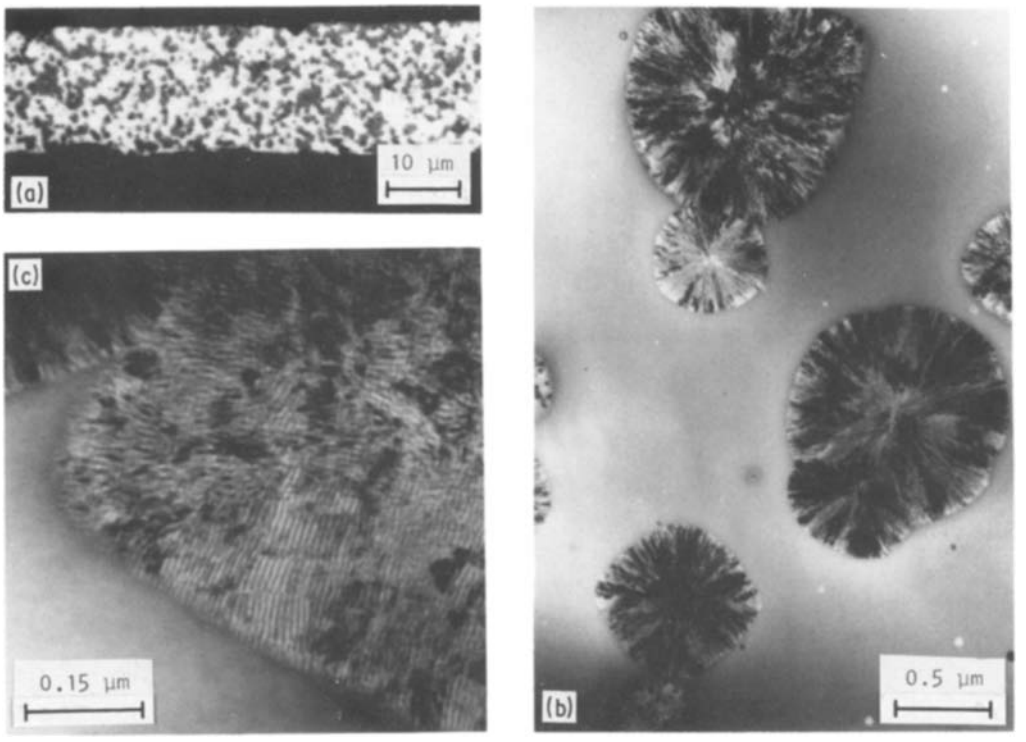

Figure 13 $Fe_{68}Cr_{10}P_{12}Si_{10}$ ribbon isothermally annealed at 773 K for 0.5 h. Crystallization product is uniformly distributed throughout the cross-section of the ribbon (a), and appears two-phase (b) and (c).

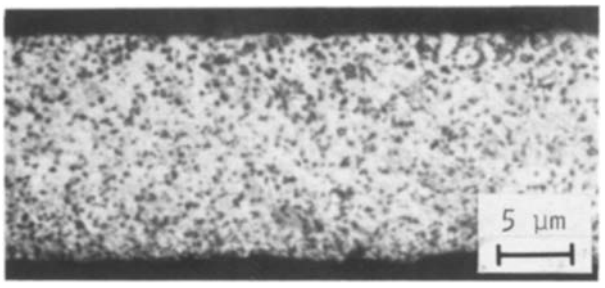

Figure 14 $Fe_{68}Si_{16}B_{16}$ ribbon isothermally annealed at 763 K for 1 h.

case there was evidence of substantial crystallization from both ribbon surfaces, together with transformation in the bulk (Figs 16 and 17). This type of surface crystallization has been reported previously for other metallic glasses [31, 32] but not, as far as we are aware, for iron-based systems. The crystallization product again appeared two-phase in each case.

In the early stages of transformation, particularly at low annealing temperatures, surface crystallization dominates, leading to n values close to two as would be expected for a one-dimensional, interface-controlled process with constant nucleation rate [33]. With increasing volume fraction transformed, the contribution to the overall kinetics from transformation within the bulk increases, shifting the mean value of n to larger values, presumably because the incubation period for surface crystallization is much shorter than that for crystallization within the bulk. At higher temperatures, the difference between incubation periods for the bulk and surface is less pronounced and the fraction of material transformed in the bulk relative to the surface increases, leading to higher mean values of Avrami coefficient.

It is interesting to note that surface crystallization of these alloys is not the result of quenched-in nuclei arising from the melt-spinning process. Fig. 18 shows optical micrographs of cross-sections through samples of a ribbon of $Fe_{72}Si_{10}B_{18}$ which were isothermally annealed at 803 K for 60 min. Fig. 18a shows the complete ribbon cross-section, including a surface formed by fracture before annealing, and Fig. 18b shows a ribbon from which the top surface had been removed by grinding immediately prior to the annealing treatment. Growth of the surface layer of crystals is identical in each case, suggesting that, although the surfaces of the ribbon are clearly preferred growth sites, this is not the result of the melt-spinning process *per se*. The reason why some alloy compositions are susceptible to this type of surface crystallization while others are not is still unresolved.

The results for the $Fe_{72}Si_{10}B_{18}$ alloy are perhaps the most convincing evidence that the application of the JMA analysis without complementary metallographic work can result in a misleading interpretation of the transformation kinetics. For each temperature, the mean value of n is close to 3 and the correlation coefficients from a least-squares analysis for $0.1 < V_f < 0.9$ are better than 0.99. The Calka plot, however, shows clearly that n varies continuously with V_f, indicating, together with the metallographic work, that the mean Avrami exponent of 3.0 is due to contributions from both surface and bulk crystallization rather than representing a true kinetic parameter. The comparison of the results from this alloy with those from $Fe_{68}Si_{16}B_{16}$, which also gives a mean n value of three, emphasizes the problems involved in using a mean value of the Avrami exponent as an indicator of transformation mechanisms.

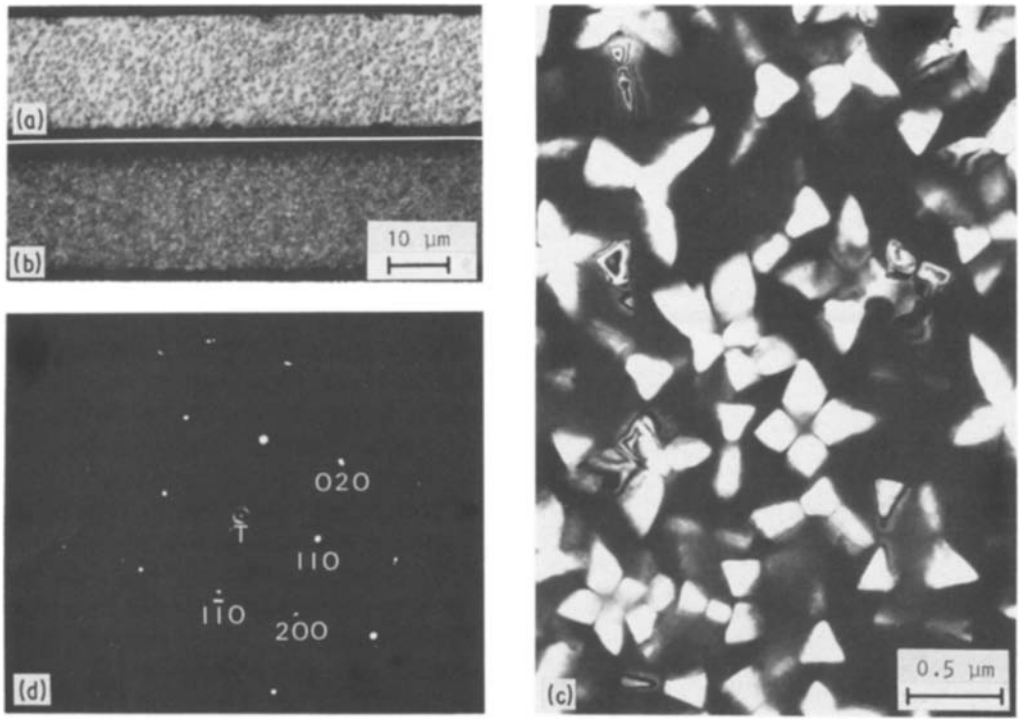

Figure 15 $Fe_{80}Si_{10}B_{10}$ ribbon, (a) isothermally annealed at 623 K for 120 h (after first crystallization peak), (b) isothermally annealed at 723 K for 120 h (after second peak), (c) dendrites formed after annealing into first peak, (d) diffraction pattern from a single α-Fe dendrite in (c).

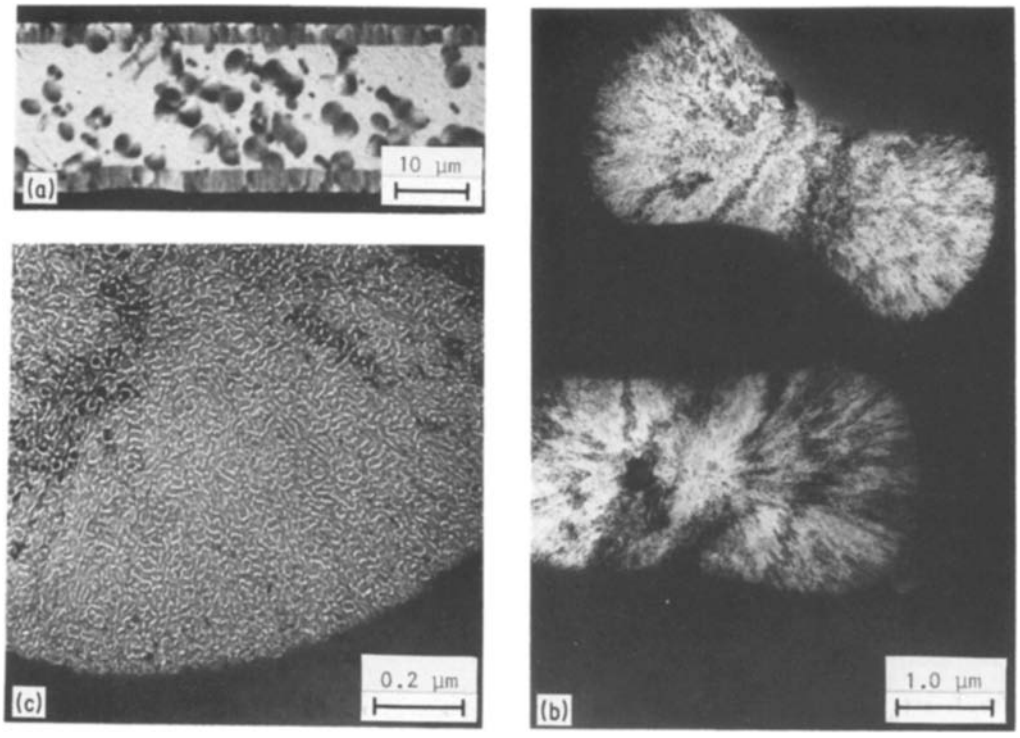

Figure 16 $Fe_{70}Cr_{10}P_{13}B_7$ ribbon isothermally annealed at 712 K for 1 h. (a) Crystallization from both surfaces and within the bulk. (b) and (c) Two-phase structure.

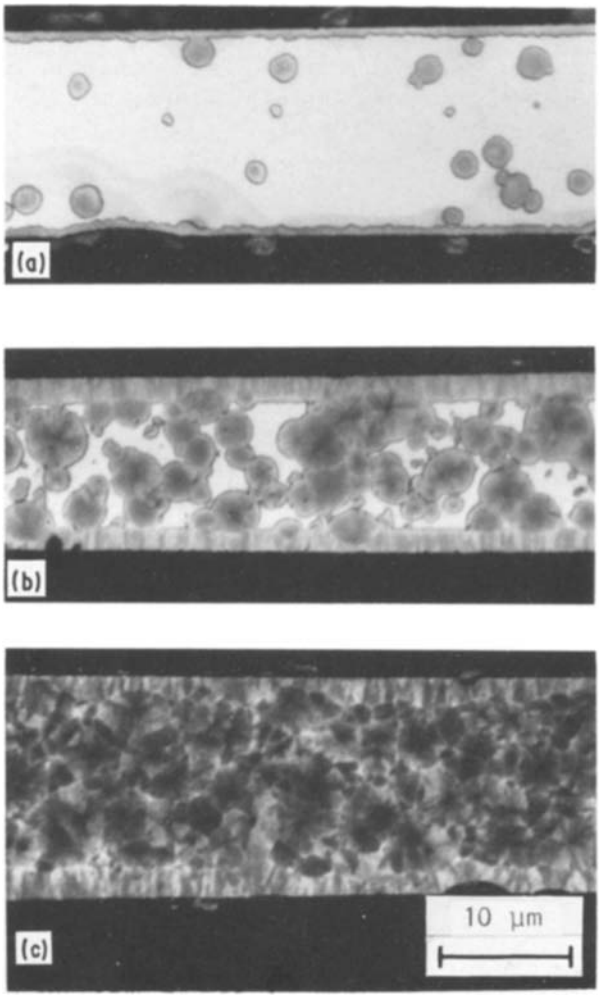

Figure 17 $Fe_{72}Si_{10}B_{18}$ ribbon annealed at 793 K for (a) 1 h, (b) 2 h, and (c) 3 h.

5. Conclusions

The conventional procedure for deducing mechanisms of transformation by calculating mean values of the Avrami exponent from the Johnson–Mehl–Avrami analysis can be misleading. The method suggested by Calka and Radlinski [9], in conjunction with detailed metallography, is a more sensitive and reliable approach. When applied to a series of iron-based metallic glasses in this investigation, only those alloys

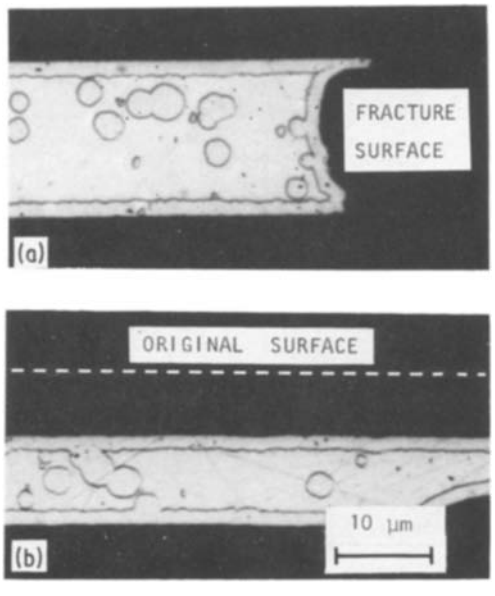

Figure 18 $Fe_{72}Si_{10}B_{18}$ ribbon annealed at 803 K for 1 h. (a) Full cross-section with transverse surface formed by fracture immediately prior to heat treatment, (b) free surface removed by grinding immediately prior to heat treatment. The extent of surface crystallization is the same in all cases.

which crystallized uniformly within the bulk of the material by a single growth process gave values of the Avrami exponent which were independent of transformation temperature and volume fraction transformed, and which were readily interpretable from the theory.

The wide variation in values of the Avrami exponent reported in the literature for apparently similar glassy alloys may be due, in part, to undetected surface crystallization effects and/or multiple crystallization processes occurring simultaneously during the transformation.

Acknowledgements

We thank Drs A. Calka and A. P. Radlinski for the opportunity to see their results [9] prior to publication.

References

1. P. DUHAZ, D. BARACOK and A. ONDREJKA, *J. Non-Cryst. Solids* **21** (1976) 411.
2. A. LUCCI and L. BATTEZZATI, *Thermochim. Acta* **54** (1982) 343.
3. C. V. THOMPSON, A. L. GREER and F. SPAEPEN, *Acta Metall.* **31** (1983) 1883.
4. K. JANSSON, M. NYGREN and A. OSTLUND, *Mater. Res. Bull.* **19** (1984) 1091.
5. E. H. HENNINGER and D. S. EASTON, *J. Mater. Sci.* **20** (1985) 4298.
6. G. K. DEY and S. BANERJEE, *Mater. Sci. Engng* **76** (1985) 127.
7. G. K. DEY, E. G. BABURAJ and S. BANERJEE, *J. Mater. Sci.* **21** (1986) 117.
8. Q. C. WU, M. HARMELIN, J. BIGOT and G. MARTIN, *ibid.* **21** (1986) 3581.
9. A. CALKA and A. P. RADLINSKI, in Proceedings of Fall Meeting 1986 Materials Research Society, Boston, Massachusetts, December 1986. To be published in "Science and Technology of Rapidly Quenched Alloys", Vol. 80, edited by M. Tenhover, L. E. Tanner and W. L. Johnson, (1987).
10. Z. Y. CAO, H. U. FRITSCH and H. W. BERGMANN, *Thermochim. Acta* **83** (1985) 23.
11. M. G. SCOTT and P. RAMACHANDRARAO, *Mater. Sci. Engng* **29** (1977) 137.
12. M. G. SCOTT, *J. Mater. Sci.* **13** (1978) 291.
13. P. H. SHINGU, Y. KOMATSU and R. OZAKI, *Suppl. Sci. Rep. RITU* **28A** (1980) 76.
14. J. WANG, S. WEI, B. DING and S. LI, in "Proceedings of the 4th International Conference on Rapidly Quenched Metals", Sendai, 1981, edited by T. Masumoto and R. Suzuki (Japan Institute Metals, Sendai, 1982) p. 731.
15. A. L. GREER, *Acta Metall.* **30** (1982) 171.
16. V. R. V. RAMANAN and G. E. FISH, *J. Appl. Phys.* **53** (3) (1982) 2273.
17. C. F. CHANG and J. MARTI, *J. Mater. Sci.* **18** (1983) 2297.
18. E. G. BABURAJ, G. K. DEY, M. J. PATNI and R. KRISHNAN, *Scripta Metall.* **19** (1985) 305.
19. K. RUSSEN, S. BUDUROV and L. ANESTIEV, in "Proceedings of the 5th International Conference on Rapidly Quenched Metals", Wurzburg, 1985, edited by S. Steeb and H. Warlimont (Elsevier, The Netherlands, 1985) p. 283.
20. D. AKHTAR, *Scripta Metall.* **20** (1986) 983.
21. C. KIM, T. KIM and M. TAKAHASHI, in "Proceedings of the 4th International Conference on Rapidly Quenched Metals", Sendai, 1981, edited by T. Masumoto and R. Suzuki (Japan Institute of Metals, Sendai, 1982), p. 723.
22. J. OREHOTSKY and C. ROWLANDS, *J. Appl. Phys.* **53** (1982) 7783.
23. T. SOUMURA, S. SAITO, I. FUJIMORI, I. MATSUMARU and T. MAEDA, *J. Mater. Sci. Lett.* **5** (1986) 216.
24. G. A. JONES, P. BONNETT and S. F. H. PARKER, *J. Mag. Mag. Mater.* **58** (1986) 216.
25. A. S. SCHAAFSMA, H. SNIJDERS, F. VAN DER WOUDE, J. W. DRIJVER and S. RADELAAR, *Phys. Rev. B* **20** (1979) 4423.
26. R. S. TIWARI, S. RANGANATHAN and M. VON HEIMENDAHL, *Z. Metallkde* **72** (1981) H8, 563.
27. W. FERNENGEL, H. KRONMULLER, M. RAPP and Y. HE, *Appl. Phys. A* **28** (1982) 137.
28. M. A. GIBSON and G. W. DELAMORE, to be published.
29. J. W. CHRISTIAN, in "The Theory of Transformations in Metals and Alloys" (Pergamon, Oxford, 1975) p. 542.
30. A. INOUE, M. KOMURO and T. MASUMOTO, *J. Mater. Sci.* **19** (1984) 4125.
31. K. F. KELTON and F. SPAEPEN, *Acta Metall.* **33** (1985) 455.
32. A. J. DREHMAN and A. L. GREER, *ibid.* **32** (1984) 323.
33. S. RANGANATHAN and M. VON HEIMENDAHL, *J. Mater. Sci.* **16** (1981) 2401.

Received 9 March
and accepted 15 May 1987